Biological Psychiatry: Celebrating 50 Years

Archival Report

Dopamine D_1 and D_2 Receptors Differentially Regulate Rac1 and Cdc42 Signaling in the Nucleus Accumbens to Modulate Behavioral and Structural Plasticity After Repeated Methamphetamine Treatment

Genghong Tu, Li Ying, Liuzhen Ye, Jinlan Zhao, Nuyun Liu, Juan Li, Yutong Liu, Mengjuan Zhu, Yue Wu, Bin Xiao, Huidong Guo, Fukun Guo, Huijun Wang, Lin Zhang, and Lu Zhang

ABSTRACT

BACKGROUND: Methamphetamine (METH) is a highly addictive psychostimulant that strongly activates dopamine receptor signaling in the nucleus accumbens (NAc). However, how dopamine D_1 and D_2 receptors (D_1Rs and D_2Rs, respectively) as well as downstream signaling pathways, such as those involving Rac1 and Cdc42, modulate METH-induced behavioral and structural plasticity is largely unknown.

METHODS: Using NAc conditional D_1R and D_2R deletion mice, Rac1 and Cdc42 mutant viruses, and a series of behavioral and morphological methods, we assessed the effects of D_1Rs and D_2Rs on Rac1 and Cdc42 in modulating METH-induced behavioral and structural plasticity in the NAc.

RESULTS: D_1Rs and D_2Rs in the NAc consistently regulated METH-induced conditioned place preference, locomotor activation, and dendritic and spine remodeling of medium spiny neurons but differentially regulated METH withdrawal–induced spatial learning and memory impairment and anxiety. Interestingly, Rac1 and Cdc42 signaling were oppositely modulated by METH, and suppression of Rac1 signaling and activation of Cdc42 signaling were crucial to METH-induced conditioned place preference and structural plasticity but not to locomotor activation. D_1Rs activated Rac1 and Cdc42 signaling, while D_2Rs inhibited Rac1 signaling but activated Cdc42 signaling to mediate METH-induced conditioned place preference and structural plasticity but not locomotor activation. In addition, NAc D_1R deletion aggravated METH withdrawal–induced spatial learning and memory impairment by suppressing Rac1 signaling but not Cdc42 signaling, while NAc D_2R deletion aggravated METH withdrawal–induced anxiety without affecting Rac1 or Cdc42 signaling.

CONCLUSIONS: D_1Rs and D_2Rs differentially regulate Rac1 and Cdc42 signaling to modulate METH-induced behavioral plasticity and the structural remodeling of medium spiny neurons in the NAc.

Keywords: Behavioral plasticity, Cdc42, Dopamine D_1 and D_2 receptors, Methamphetamine, Nucleus accumbens, Rac1, Structural plasticity

https://doi.org/10.1016/j.biopsych.2019.03.966

Drug addiction is a chronic disease with a high relapse rate and is characterized by compulsive drug seeking and strong withdrawal symptoms (1). Addictive drugs, such as methamphetamine (METH), can augment the dopamine level in the nucleus accumbens (NAc) (2–5), triggering the signaling pathway downstream of the dopamine receptors (6).

Drug-induced behavioral plasticity is a series of long-lasting behavioral changes that occur after repeated administration (7,8). In the NAc region, the dopamine D_1 and D_2 receptors (D_1Rs and D_2Rs, respectively) are primarily distributed in distinct medium spiny neurons (MSNs), which are subdivided into D_1R-expressing MSNs (D_1-MSNs) and D_2R-expressing MSNs (D_2-MSNs) (9). D_1R activation in the medial prefrontal cortex positively regulates METH-induced hyperactivity (10) and intraperitoneal injection of a D_1R inhibitor but not a D_2R inhibitor before METH self-administration training can reduce drug-seeking behavior (11). Conditional knockdown of D_2Rs in the NAc core attenuates METH-induced conditioned place preference (CPP) and locomotor sensitization (12). Moreover, systemic inhibition of D_1Rs and D_2Rs suppresses the expression of METH-induced CPP (13). Meanwhile, drug withdrawal causes a long-lasting decrease in mesolimbic dopamine signaling, and both D_1Rs and D_2Rs are involved (14,15). These persistent changes may underlie withdrawal syndromes, such

 © 2019 Society of Biological Psychiatry.
 ISSN: 0006-3223

as anxiety and impairment of spatial learning and memory (16–18). The above studies indicate the important roles of D_1Rs and D_2Rs in mediating METH-associated behaviors.

Psychostimulants can induce the structural remodeling of MSNs in the NAc by increasing the length and complexity of dendrites, enhancing spine density, and reshaping spine morphology (19–22). Although the molecular mechanisms of drug-induced structural plasticity have attracted widespread attention (23–25), they are not fully understood, especially those related to METH. D_1Rs and D_2Rs are critical for the dendritic and spine remodeling induced by addictive substances (26–28). D_1R promotes the increases in dendritic branching and spine density that are induced by cocaine, and although D_2R has no effect on changes in dendritic branching, it is involved in the regulation of dendritic density (28). In addition, signaling of the Rho guanosine triphosphatase (GTPase) family members Rac1 and Cdc42 is closely related to dendritic growth and spine remodeling (29–34). Bidirectional stimulation of Rac1 in the NAc and the caudate putamen modulates cocaine-induced spine remodeling (20,35), and Cdc42 expression is significantly increased after alcohol withdrawal (36). Moreover, dopamine receptors participate in a variety of biological processes, such as active forgetting, dendritic remodeling, and gene expression, by regulating Rho family GTPases (37–39). These data suggest the involvement of dopamine receptors and Rho family GTPases in METH addiction.

In this study, using NAc conditional D_1R and D_2R deletion mice and Rac1 and Cdc42 mutant viruses, we found that D_1Rs and D_2Rs differentially regulate Rac1 and Cdc42 signaling to modulate METH-induced behavioral and structural plasticity. Our findings suggest that the transmission of dopamine receptor signals to downstream molecules, such as Rac1 and/or Cdc42, may serve as a therapeutic target for the treatment of drug addiction.

METHODS AND MATERIALS

For detailed methods and materials, please see the Supplement. Briefly, adult male and female wild-type (WT) mice, *Drd1*$^{loxp/loxp}$ mice, and *Drd2*$^{loxp/loxp}$ mice on a C57BL/6J background were microinjected with the Cre and Rac1/Cdc42 mutant viruses to conditionally knock out D_1R/D_2R and/or modulate Rac1/Cdc42 activity in the NAc. A series of behavioral experiments were performed, including CPP, locomotor activity, open field test (OF), elevated plus maze (EPM), and Morris water maze (MWM) tests. For dendrite and spine quantitation, MSNs were intracellularly injected with Lucifer yellow (LY) or labeled with the Cre and/or Rac1/Cdc42 mutant viruses expressing enhanced green fluorescent protein (EGFP)/mCherry.

RESULTS

Low-Dose METH Induces Behavioral and Structural Plasticity Without Causing Neurotoxicity

To assess the behavioral consequences after treatment with METH, we conducted CPP and locomotor activity experiments. We found that the mice treated with METH (2 mg/kg) had significantly higher CPP scores and locomotor activity than those in the saline group. However, the locomotor activity of mice treated with METH was not significantly increased with time (Figure 1A–D). METH is not only highly addictive but also strongly neurotoxic, and its neurotoxic properties are dose dependent (40). Here, we found that the rewarding effect of METH at the 2 mg/kg dose was strong but nontoxic, as no apoptotic neurons were observed (Figure 1K), and the neuronal structure was normal (Figure 1L) in brain regions related to the dopaminergic circuit.

To verify whether 2 mg/kg METH can induce structural remodeling in the NAc, the mice were immediately anesthetized and intracardially perfused after the CPP test, and coronal sections of the NAc were then collected. Using intracellular injection of LY, we clearly observed that the dendritic branches were longer and more complex and the total spines, and especially the thin and mushroom spines were denser in the METH CPP group (Figure 1E–J). The soma size of MSNs was not affected after METH treatment (Supplemental Figure S1). Meanwhile, partial correlation analyses showed that the total spine density were positively correlated with the METH-induced CPP (Supplemental Figure S2).

D_1Rs and D_2Rs in the NAc Are Associated With METH-Induced Behavioral and Structural Plasticity

Dopamine receptor signaling can be activated after METH treatment (11–13), but evidence related to the precise roles of D_1Rs and D_2Rs in the NAc in METH-induced behavioral plasticity is very limited. We first induced NAc-specific deletion of D_1Rs (NAc Drd1KO) and D_2Rs (NAc Drd2KO) by bilaterally injecting adeno-associated virus serotype 2/8 vectors expressing the Cre enzyme into the NAc area of *Drd1*$^{loxp/loxp}$ and *Drd2*$^{loxp/loxp}$ mice, respectively. Immunofluorescence staining of coronal sections from NAc Drd1KO mice and NAc Drd2KO mice confirmed the deletion of D_1Rs and D_2Rs in the area of the NAc infected with the Cre virus but not in the uninfected area (Figure 2C). In addition, the viruses were expressed only in the NAc, without affecting other brain regions (Supplemental Figure S3). Behaviorally, both NAc Drd1KO mice and NAc Drd2KO mice had lower CPP scores than WT mice in the METH CPP group (Figure 2D). In addition, the basal locomotion of NAc Drd2KO mice tended to decrease. Compared with that of WT mice treated with METH, the locomotion of NAc Drd1KO mice and NAc Drd2KO mice was significantly decreased (Figure 2E). These results suggest that both D_1Rs and D_2Rs in the NAc are involved in the METH-induced CPP and locomotor activation.

To determine whether D_1Rs and D_2Rs modulate METH withdrawal–induced behaviors, the OF and EPM tests were used to assess anxiety-related behaviors (41,42), and the MWM was used to assess spatial learning and memory (Figure 2F) (43). Our results showed that the central distance, time spent in the open arms, and number of entries into the open arms were reduced in WT, NAc Drd1KO, and NAc Drd2KO mice 7 days after METH withdrawal. Additionally, compared with those in METH-treated WT mice, these three parameters were further reduced in METH-treated NAc Drd2KO mice (Figure 2H–J). The total distance traveled by each group was unaffected (Figure 2G). NAc Drd1KO mice treated with saline exhibited longer escape latencies and fewer platform crossings than WT mice. Additionally, NAc Drd1KO

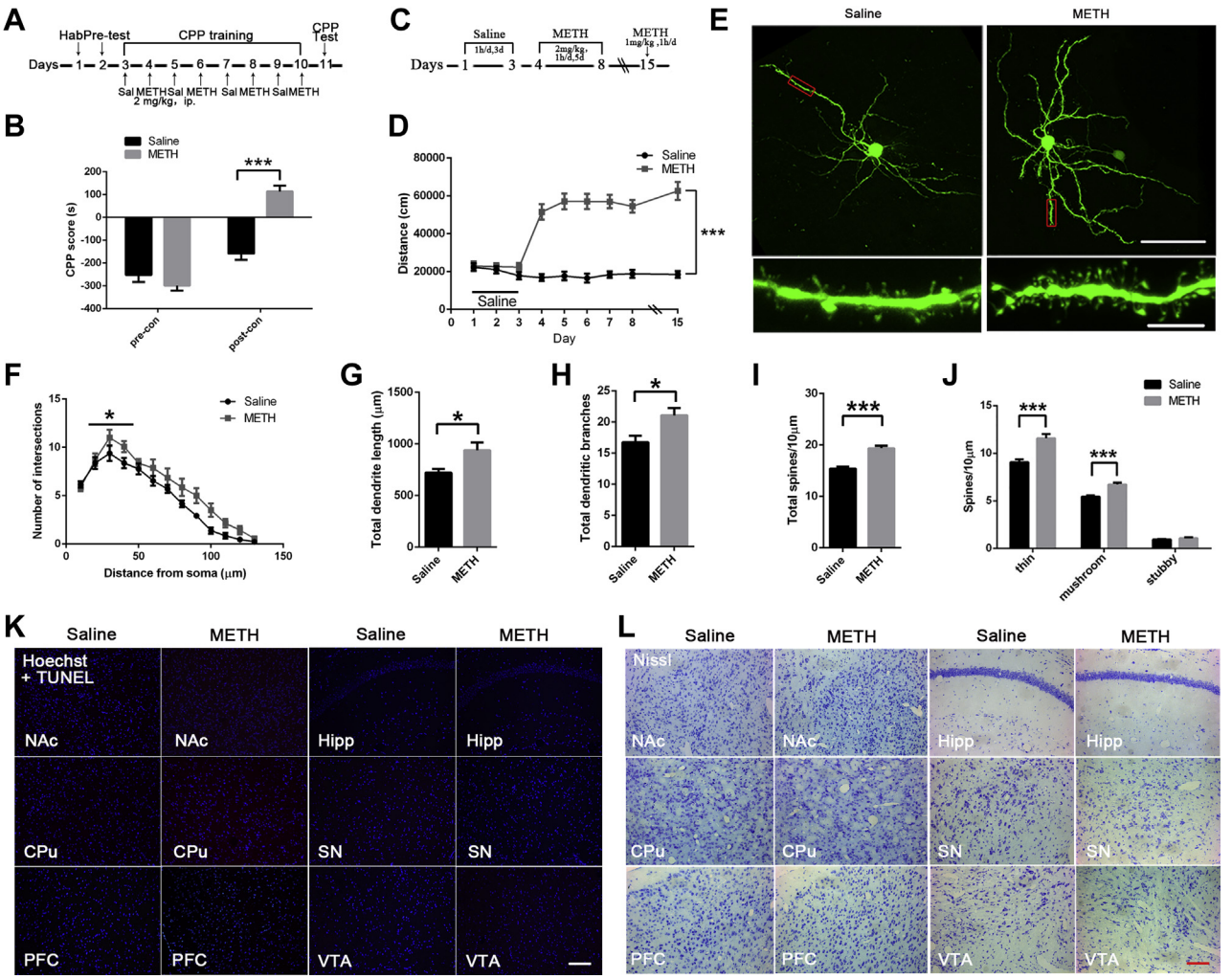

Figure 1. Low-dose methamphetamine (METH) induces behavioral and structural plasticity without causing neurotoxicity. **(A–D)** Low dose of METH (2 mg/kg) induced **(A, C)** conditioned place preference (CPP) and **(B, D)** locomotor activation (CPP: n = 12 mice/group; locomotion: n = 9 or 10 mice/group). **(E)** Representative morphology of medium spiny neurons in the nucleus accumbens (NAc) in saline (Sal) and METH CPP mice (n = 4 mice/group). Mice were immediately anesthetized and intracardially perfused after CPP test, and then the coronal sections containing NAc were collected for microinjection of Lucifer yellow. The images were obtained by confocal scanning at the specific excitation wavelength (405 nm) of Lucifer yellow. Scale bar = 50 μm or 5 μm. **(F–H)** The dendrites of medium spiny neurons in the NAc were more complex, and the dendritic lengths and branch number were increased in METH CPP mice (n = 13 or 15 neurons/group, sampled from 4 mice/treatment condition). **(I, J)** The density of the total spines in the NAc, especially of the thin and mushroom spines, was significantly increased in the METH CPP mice (n = 48 dendrites/group, sampled from 4 mice/treatment condition). **(K, L)** No apoptotic neurons or aberrant morphology was observed in the NAc, caudate putamen (CPu), prefrontal cortex (PFC), hippocampus (Hipp), substantia nigra (SN), or ventral tegmental area (VTA) between the Sal and METH CPP mice (n = 12 segments/group, sampled from 3 mice/treatment condition). Scale bar = 100 μm. The data are shown as mean ± SEM. *$p < .05$; ***$p < .001$. Hab, habituation; ip, intraperitoneal; TUNEL, terminal deoxynucleotidyl transferase mediated dUTP nick end labeling.

mice, but not NAc Drd2KO mice, exhibited increased escape latencies and a decreased number of platform crossings compared with WT mice after 7 days of METH withdrawal (Figure 2K–N). These results suggest that while NAc D_1R deletion exacerbated METH withdrawal–induced spatial learning and memory impairment, NAc D_2R deletion aggravated anxiety-related behaviors.

As structural plasticity is correlated with METH- and cocaine-induced CPP (44,45), we considered whether conditional D_1R or D_2R deletion would also affect the METH-induced structural remodeling. The mice were anesthetized and intracardially perfused immediately after the CPP test. Brain tissues containing the NAc were cut into coronal sections for morphological experiments. Compared with those of the corresponding WT mice, the dendritic complexity and length, the branch number and total spine density of NAc Drd1KO mice and NAc Drd2KO mice were significantly suppressed in the METH CPP groups but were unaffected in the saline CPP groups (Figure 3A–H). Conditional knockout of D_1R or D_2R in the NAc reduced the METH-induced increases in the thin and mushroom spine densities, whereas the stubby spine density was unaffected (Figure 3I–K). These results indicate that D_1Rs and D_2Rs in the NAc consistently regulate structural remodeling, which is correlated with METH-induced CPP.

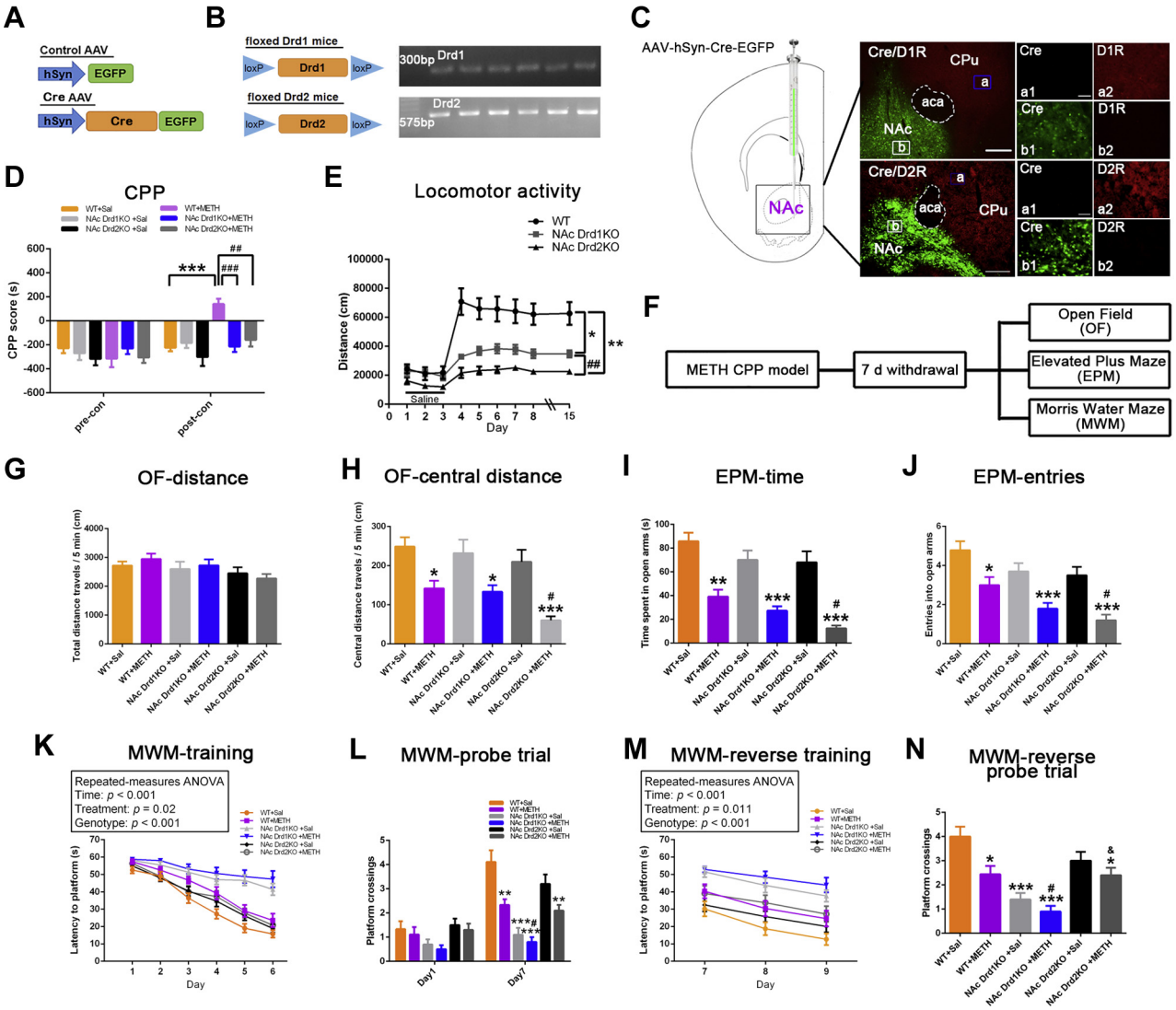

Figure 2. Dopamine D_1 and D_2 receptors (D_1Rs and D_2Rs, respectively) in the nucleus accumbens (NAc) are associated with methamphetamine (METH)-induced behavioral plasticity. **(A)** A schematic diagram of the viral vectors used in this experiment. **(B)** Polymerase chain reaction identification of homozygous *Drd1*$^{loxp/loxp}$ and *Drd2*$^{loxp/loxp}$ mice. **(C)** Immunofluorescence staining of coronal sections from *Drd1*$^{loxp/loxp}$ and *Drd2*$^{loxp/loxp}$ mice showed that D_1Rs and D_2Rs were deleted after infection with Cre viral vectors in the NAc. Scale bar = 200 μm or 50 μm. **(D, E)** Conditional knockout of D_1R or D_2R in the NAc (NAc Drd1KO and NAc Drd2KO, respectively) suppressed METH-induced conditioned place preference (CPP) and locomotor activation (CPP: n = 10 mice/group; locomotion: n = 9 or 10 mice/group). **(F)** A schematic diagram of the experimental design for the open field (OF), elevated plus maze (EPM), and Morris water maze (MWM) tests (n = 9 or 10 mice/group). **(G–J)** The deletion of D_2R in the NAc aggravated anxiety-related behavior after METH withdrawal. **(K–N)** The deletion of D_1R in the NAc per se impaired spatial learning and memory. In addition, the deletion of D_1R in the NAc further exacerbated the spatial learning and memory impairment induced by METH withdrawal. The data are shown as mean ± SEM. Compared with wild-type (WT) + saline (Sal) group: $^{*}p < .05$, $^{**}p < .01$, $^{***}p < .001$; compared with WT + METH group: $^{\#}p < .05$, $^{\#\#}p < .01$, $^{\#\#\#}p < .001$; compared with NAc Drd1KO + METH group: $^{\&}p < .05$. Locomotion: compared with WT group: $^{*}p < .05$, $^{**}p < .01$; compared with NAc Drd1KO group, $^{\#\#}p < .01$. AAV, adeno-associated virus; ANOVA, analysis of variance; EGFP, enhanced green fluorescent protein.

METH Differentially Regulates Rac1 and Cdc42 Signaling to Mediate Behavioral and Structural Plasticity

To investigate whether Rac1 and Cdc42 signaling in the NAc were affected by repeated METH treatment, we immediately collected NAc specimens after the CPP test. The results showed that Rac1 signaling, including Rac1 activity and p21 (Rac1) activated kinase 1 (PAK1) phosphorylation, was suppressed. Interestingly, however, Cdc42 signaling, including Cdc42 activity and neural Wiskott–Aldrich syndrome protein (N-WASP) phosphorylation was augmented in the METH CPP group. The expression levels of total Rac1, PAK1, Cdc42, and N-WASP were unaffected (Figure 4A–D).

To evaluate the effects of Rac1 and Cdc42 on METH-induced behavioral and structural plasticity, lentiviruses

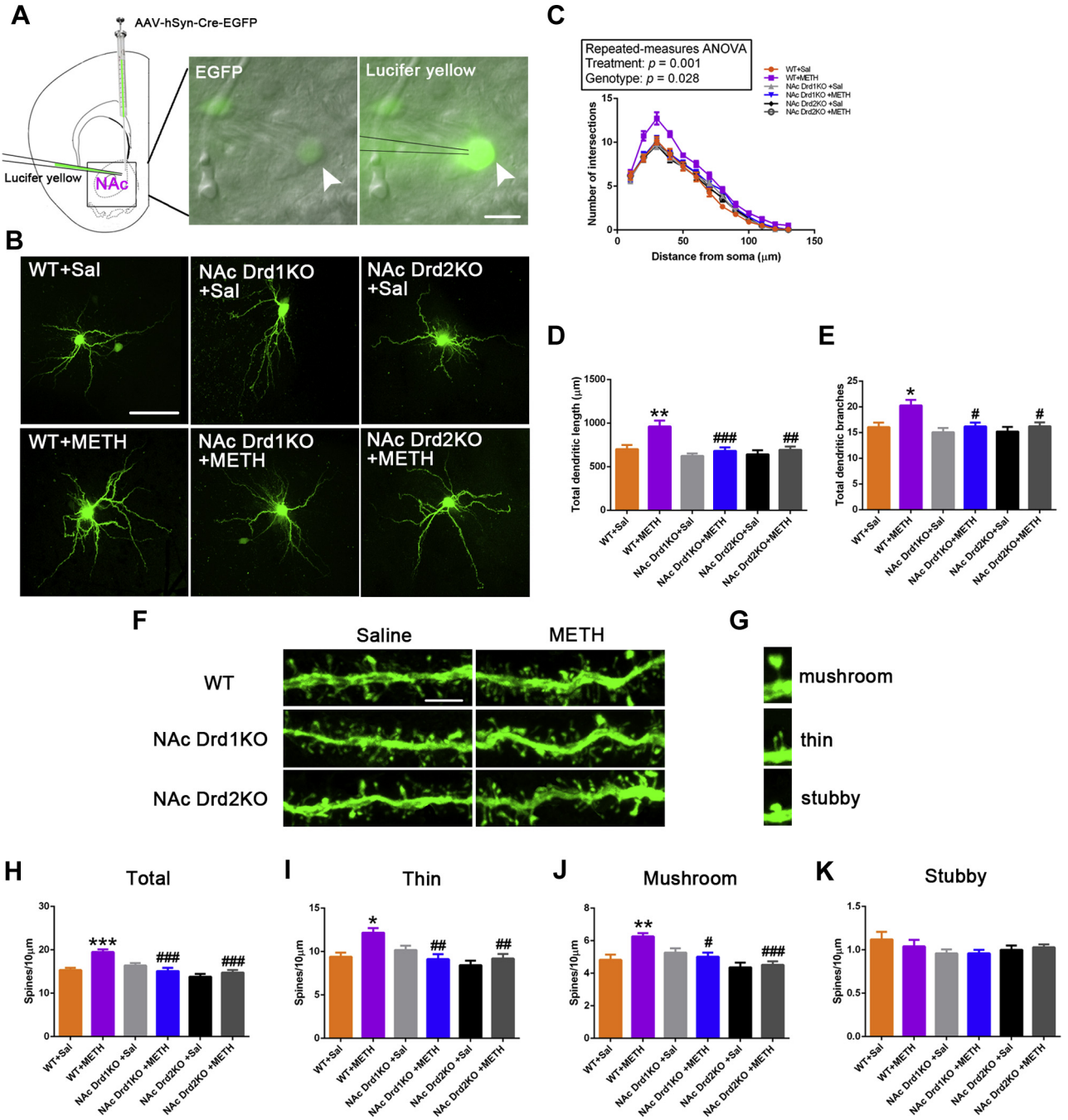

Figure 3. Conditional knockout of dopamine D_1 or D_2 receptor (D_1R and D_2R, respectively) in the nucleus accumbens (NAc Drd1KO and NAc Drd2KO, respectively) suppresses methamphetamine (METH)-induced structural plasticity. **(A)** A schematic diagram of Lucifer yellow intracellular injection experiment. The mice were stereotactically infected with adeno-associated virus (AAV) expressing Cre or enhanced green fluorescent protein (EGFP) (negative control) in the NAc. Three weeks after the infection, the mice were assigned to saline (Sal) conditioned place preference (CPP) or METH CPP. The mice were immediately anesthetized and intracardially perfused after the CPP test and coronal sections containing the NAc were then collected for intracellular injection of Lucifer yellow. Only medium spiny neurons (MSNs) expressing EGFP in the NAc were selected, as the arrowheads show. Scale bar = 10 μm. **(B)** Representative morphology of MSNs in each group. (n = 15–18 neurons/group, sampled from 3 mice/treatment condition). The images were obtained by confocal scanning at the specific excitation wavelength (405 nm) of Lucifer yellow. Scale bar = 50 μm. **(C–E)** Conditional knockout of D_1R and D_2R in the NAc blocked METH-induced increases in dendritic complexity, dendritic length, and branch number of MSNs in the NAc. **(F)** Representative images of spine remodeling in the three strains of mice after saline CPP and METH CPP. Scale bar = 5 μm. **(G)** Representative morphology of the spines. **(H–K)** Conditional knockout of D_1R and D_2R in the NAc blocked the ability of METH to increase the spine density of MSNs, an effect that was primarily driven by the decreases in the densities of thin and mushroom spines (n = 27–48 dendrites/group, sampled from 4 mice/treatment condition). The data are shown as mean ± SEM. Compared with wild-type (WT) + Sal group: $^{*}p < .05$, $^{**}p < .01$, $^{***}p < .001$; compared with WT + METH group: $^{\#}p < .05$, $^{\#\#}p < .01$, $^{\#\#\#}p < .001$. ANOVA, analysis of variance.

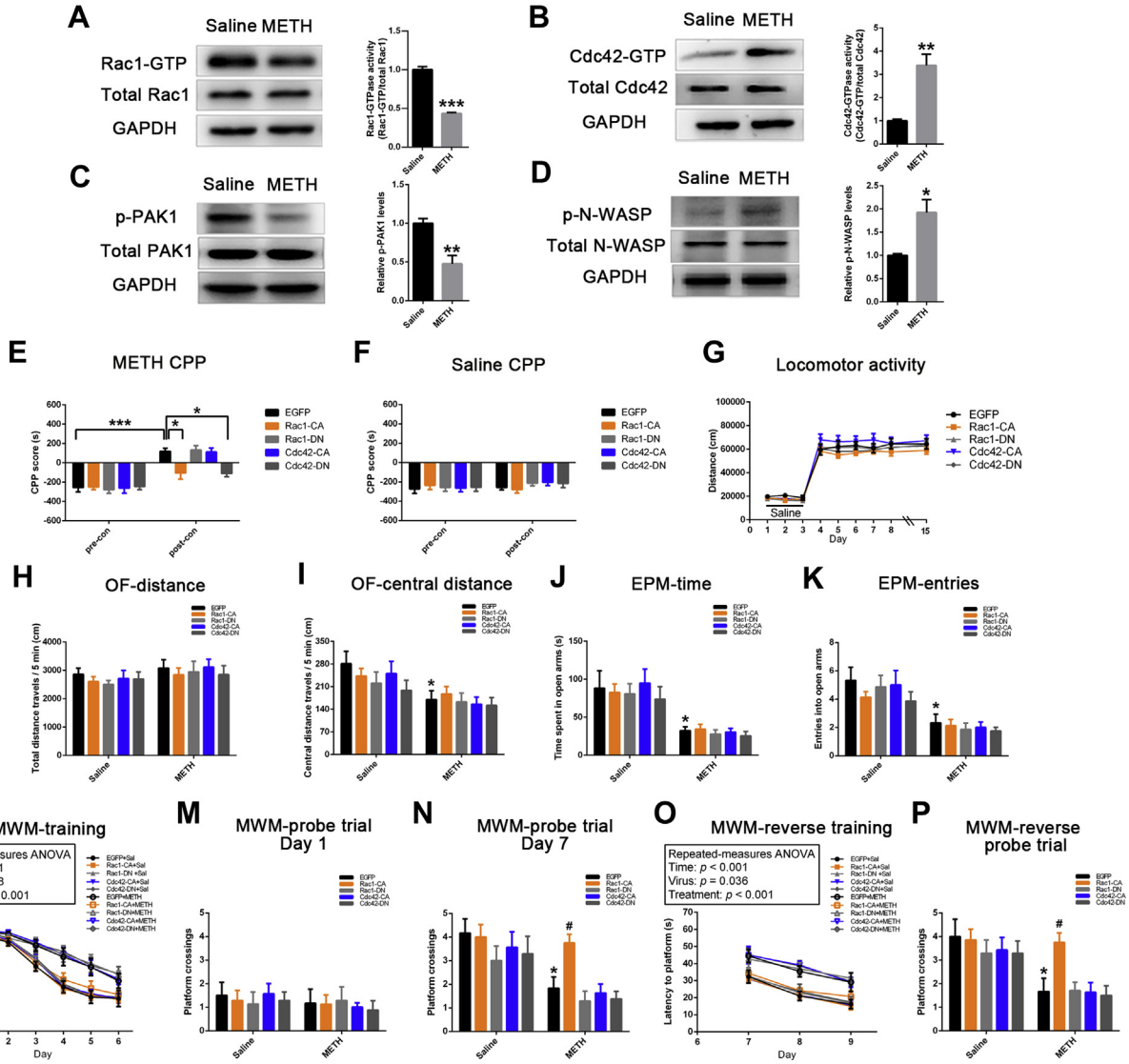

Figure 4. Methamphetamine (METH) differentially regulates Rac1 and Cdc42 signaling to mediate behavioral plasticity. **(A–D)** Rac1 activity (Rac1-guanosine triphosphate [GTP]) and phosphorylated p21 (Rac1) activated kinase 1 (p-PAK1) were decreased in METH conditioned place preference (CPP) mice without affecting total Rac1 or PAK1 levels, while Cdc42 activity (Cdc42-GTP) and phosphorylated neural Wiskott–Aldrich syndrome protein (p-N-WASP) were enhanced in METH CPP mice without affecting total Cdc42 or N-WASP levels (n = 4 mice/group). The data are shown as mean ± SEM. Compared with the group of saline (Sal): $^{*}p < .05$, $^{**}p < .01$, $^{***}p < .001$. **(E–P)** The mice were stereotactically infected with lentiviruses expressing a constitutively active (L61) or dominant-negative (N17) mutant of Rac1 (Rac1-CA and Rac1-DN, respectively), a constitutively active (L61) or dominant-negative (N17) mutant of Cdc42 (Cdc42-CA and Cdc42-DN, respectively), or a negative control (enhanced green fluorescent protein [EGFP]) in the nucleus accumbens (NAc). Two weeks after infection, the mice were assigned to CPP (n = 6–8 mice/group) or locomotor activity (n = 6–7 mice/group). The mice assigned to CPP continued to the open field (OF), elevated plus maze (EPM), and Morris water maze (MWM) tests after 7 days of METH withdrawal. **(E)** Rac1-CA and Cdc42-DN mice showed lower CPP scores than EGFP mice exposed to METH CPP. The data are shown as mean ± SEM. $^{*}p < .05$, $^{**}p < .01$, $^{***}p < .001$. **(F)** None of the viral vectors had any effect on natural preference. **(G-K)** Rac1-CA and Cdc42-DN had no effect on **(G)** METH-induced locomotor activation or **(H–K)** METH withdrawal–induced anxiety-related behavior. **(L–P)** Only Rac1-CA alleviated METH withdrawal–induced spatial learning and memory impairment. The data are shown as mean ± SEM. Compared with EGFP + Sal group: $^{*}p < .05$; compared with EGFP + METH group: $^{\#}p < .05$. ANOVA, analysis of variance; GAPDH, glyceraldehyde 3-phosphate dehydrogenase.

expressing a constitutively active (L61) or dominant-negative (N17) mutant of Rac1 (Rac1-CA and Rac1-DN, respectively), a constitutively active or dominant-negative mutant of Cdc42 (Cdc42-CA and Cdc42-DN, respectively), or an EGFP vector were individually stereotactically injected into the NAc. We found that compared with the EGFP, Rac1-CA and Cdc42-DN significantly decreased the CPP scores in the METH CPP groups (Figure 4E). After METH CPP training, the mice were subjected to the OF, EPM, and MWM tests. The results of the MWM showed that only Rac1-CA shortened the escape latencies and increased the number of platform crossings after 7 days of METH withdrawal (Figure 4L–P). None of the viral

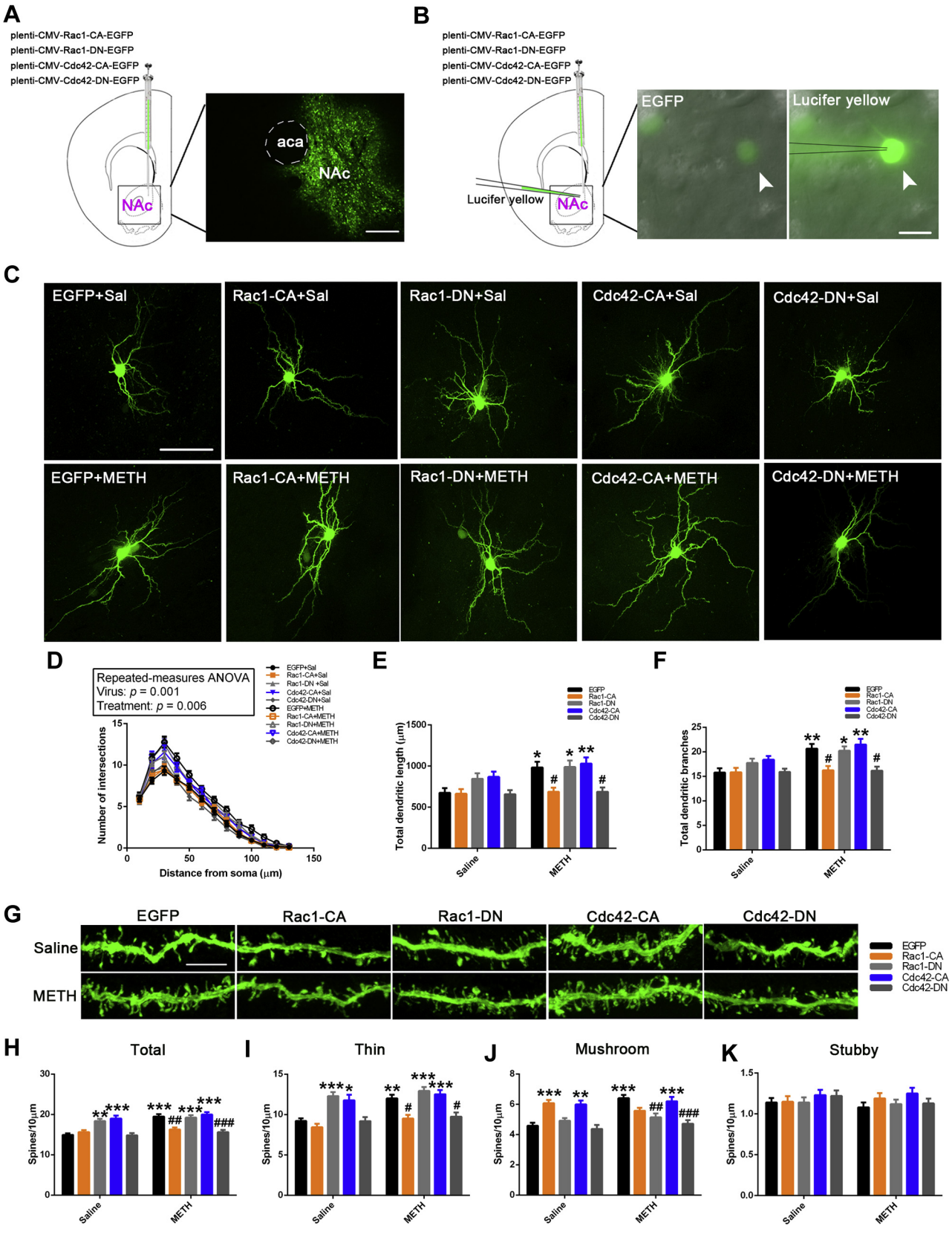
A
plenti-CMV-Rac1-CA-EGFP
plenti-CMV-Rac1-DN-EGFP
plenti-CMV-Cdc42-CA-EGFP
plenti-CMV-Cdc42-DN-EGFP
NAc
aca
NAc
B
plenti-CMV-Rac1-CA-EGFP
plenti-CMV-Rac1-DN-EGFP
plenti-CMV-Cdc42-CA-EGFP
plenti-CMV-Cdc42-DN-EGFP
Lucifer yellow
NAc
EGFP
Lucifer yellow
C
EGFP+Sal
Rac1-CA+Sal
Rac1-DN+Sal
Cdc42-CA+Sal
Cdc42-DN+Sal
EGFP+METH
Rac1-CA+METH
Rac1-DN+METH
Cdc42-CA+METH
Cdc42-DN+METH
D
Repeated-measures ANOVA
Virus: p = 0.001
Treatment: p = 0.006
EGFP+Sal
Rac1-CA+Sal
Rac1-DN +Sal
Cdc42-CA+Sal
Cdc42-DN+Sal
EGFP+METH
Rac1-CA+METH
Rac1-DN+METH
Cdc42-CA+METH
Cdc42-DN+METH
Number of intersections
Distance from soma (μm)
E
EGFP
Rac1-CA
Rac1-DN
Cdc42-CA
Cdc42-DN
Total dendritic length (μm)
Saline
METH
F
EGFP
Rac1-CA
Rac1-DN
Cdc42-CA
Cdc42-DN
Total dendritic branches
Saline
METH
G
EGFP
Rac1-CA
Rac1-DN
Cdc42-CA
Cdc42-DN
Saline
METH
EGFP
Rac1-CA
Rac1-DN
Cdc42-CA
Cdc42-DN
H
Total
Spines/10μm
Saline
METH
I
Thin
Spines/10μm
Saline
METH
J
Mushroom
Spines/10μm
Saline
METH
K
Stubby
Spines/10μm
Saline
METH

vectors had any effect on the saline CPP (Figure 4F). In addition, Rac1-CA and Cdc42-DN had no effect on METH-induced locomotor activation (Figure 4G) or METH withdrawal–induced anxiety-related behaviors (Figure 4H–K). These results suggest that the inactivation of Rac1 and the activation of Cdc42 are responsible for METH-induced CPP but not locomotor activation and that the inactivation of Rac1 but not the activation of Cdc42 contributes to METH withdrawal–induced spatial learning and memory impairment. Moreover, we found that Rac1 and Cdc42 activity had distinct effects on structural remodeling in the NAc. Both Rac1-CA and Cdc42-DN blocked the METH-induced increases in dendritic complexity, dendritic length, and branch number. All the viral vectors had no effect on the dendrites in the saline groups (Figure 5B–F). In the saline CPP group, both Rac1-DN and Cdc42-CA increased the total spine density; specifically, Rac1-DN largely increased thin spine density, while Cdc42-CA increased both the thin and mushroom spine densities. Although neither Rac1-CA nor Cdc42-DN affected the total spine density in the saline CPP group, compared with EGFP, Rac1-CA significantly increased the mushroom spine density under saline treatment. The total spine density was increased in the METH CPP group and was dramatically blocked by Rac1-CA and Cdc42-DN. Compared with EGFP under METH treatment, Rac1-CA reduced the thin spine density, and Cdc42-DN reduced both the thin and mushroom spine densities (Figure 5G–K).

Conditional Knockout of D_1R or D_2R in the NAc Alters METH-Induced Rac1 and Cdc42 Signaling

Dopamine receptors participate in a variety of biological processes, especially in dendritic remodeling, by regulating the Rho family GTPases (37–39). Therefore, we considered whether D_1Rs/D_2Rs regulated Rac1/Cdc42 in METH CPP mice. NAc specimens from WT, NAc Drd1KO, and NAc Drd2KO mice were collected immediately after the CPP test. Interestingly, we found that after METH CPP test, Rac1 signaling, including Rac1 activity and PAK1 phosphorylation, and Cdc42 signaling, including Cdc42 activity and N-WASP phosphorylation, were both decreased in NAc Drd1KO mice. In contrast, Rac1 signaling was increased in NAc Drd2KO mice, whereas Cdc42 signaling was decreased in METH-treated NAc

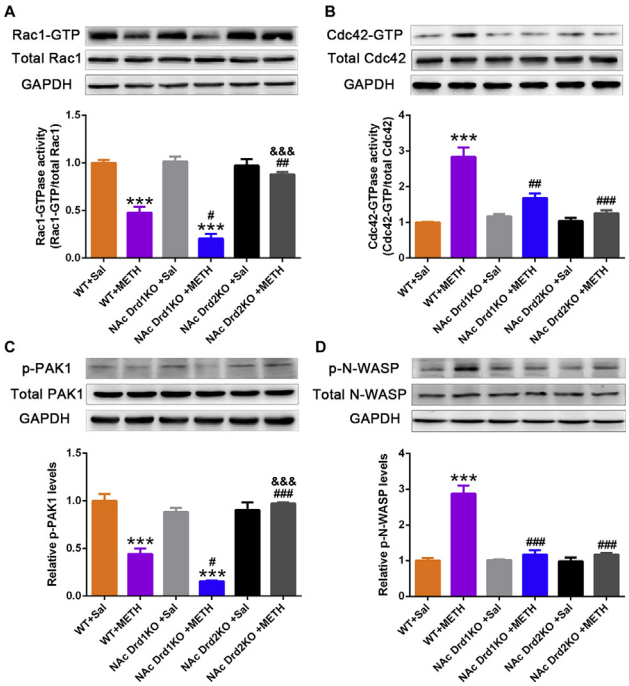

Figure 6. Conditional knockout of dopamine D_1 or D_2 receptor (D_1R and D_2R, respectively) in the nucleus accumbens (NAc Drd1KO and NAc Drd2KO, respectively) alters methamphetamine (METH)-induced Rac1 and Cdc42 signaling. NAc specimens were obtained immediately after the conditioned place preference (CPP) test (n = 3 mice/group). **(A, C)** Conditional knockout of D_1R further decreased Rac1 activity and the phosphorylation of its downstream effector p21 (Rac1) activated kinase 1 (PAK1), while conditional knockout of D_2R increased Rac1 activity and PAK1 phosphorylation after METH treatment. The expression of total Rac1 and PAK1 was unaffected in all groups. **(B, D)** Conditional knockout of D_1R or D_2R suppressed Cdc42 activity and the phosphorylation of its downstream effector neural Wiskott–Aldrich syndrome protein (N-WASP) after METH treatment. The expression of total Cdc42 and N-WASP was unaffected. The data are shown as mean ± SEM. Compared with wild-type (WT) + saline (Sal) group: $^{***}p < .001$; compared with WT + METH group: $^{\#}p < .05$, $^{\#\#}p < .01$, $^{\#\#\#}p < .001$; compared with NAc Drd1KO + METH group: $^{\&\&\&}p < .001$. ANOVA, analysis of variance; GAPDH, glyceraldehyde 3-phosphate dehydrogenase; GTP, guanosine triphosphate; p-N-WASP, phosphorylated N-WASP; p-PAK1, phosphorylated PAK1.

Figure 5. Methamphetamine (METH) differentially regulates Rac1 and Cdc42 signaling to mediate structural plasticity. **(A)** Representative image of the stereotactic injection site of the nucleus accumbens (NAc). Scale bar = 200 μm. **(B)** A schematic diagram of Lucifer yellow intracellular injection experiment. The mice were stereotactically infected with lentiviruses expressing a constitutively active (L61) or dominant-negative (N17) mutant of Rac1 (Rac1-CA and Rac1-DN, respectively), a constitutively active (L61) or dominant-negative (N17) mutant of Cdc42 (Cdc42-CA and Cdc42-DN, respectively), or enhanced green fluorescent protein (EGFP) (negative control) in the NAc. Two weeks after the infection, the mice were assigned to saline (Sal) conditioned place preference (CPP) or METH CPP. The mice were immediately anesthetized and intracardially perfused after the CPP test and coronal sections containing the NAc were then collected for intracellular injection of Lucifer yellow. Only medium spiny neurons expressing EGFP in the NAc were selected, as the arrowheads show. Scale bar = 10 μm. **(C)** Representative morphology of medium spiny neurons in each group. The images were obtained by confocal scanning at the specific excitation wavelength (405 nm) of Lucifer yellow (n = 16–19 neurons/group, sampled from 3 mice/treatment condition). Scale bar = 50 μm. **(D–F)** METH increased the dendritic complexity, dendritic length, and branch number of medium spiny neurons in the NAc, which was blocked by Rac1-CA and Cdc42-DN. **(G)** Representative images of spine remodeling in each group (n = 25–39 dendrites/group, sampled from 3 mice/treatment condition). Scale bar = 5 μm. **(H)** Rac1-DN and Cdc42-CA increased the total spine density under Sal treatment. METH increased total spine density, which was blocked by Rac1-CA and Cdc42-DN. **(I–K)** In the Sal CPP groups, Rac1-DN greatly increased thin spine density, whereas Cdc42-CA increased both the thin and mushroom spine densities. Rac1-CA significantly increased the mushroom spine density, although it had no effect on the total spine density under Sal treatment. Compared with the METH CPP group infected with EGFP, the METH CPP groups infected with Rac1-CA and Rac1-DN showed suppression of thin and mushroom spine density, respectively. The METH CPP group infected with Cdc42-DN exhibited suppression of both the thin and mushroom spine densities. None of the viral vectors had any effect on stubby spine density. The data are shown as mean ± SEM. Compared with EGFP + Sal group: $^{*}p < .05$, $^{**}p < .01$, $^{***}p < .001$; compared with EGFP + METH group: $^{\#}p < .05$, $^{\#\#}p < .01$, $^{\#\#\#}p < .001$. ANOVA, analysis of variance; CMV, cytomegalovirus.

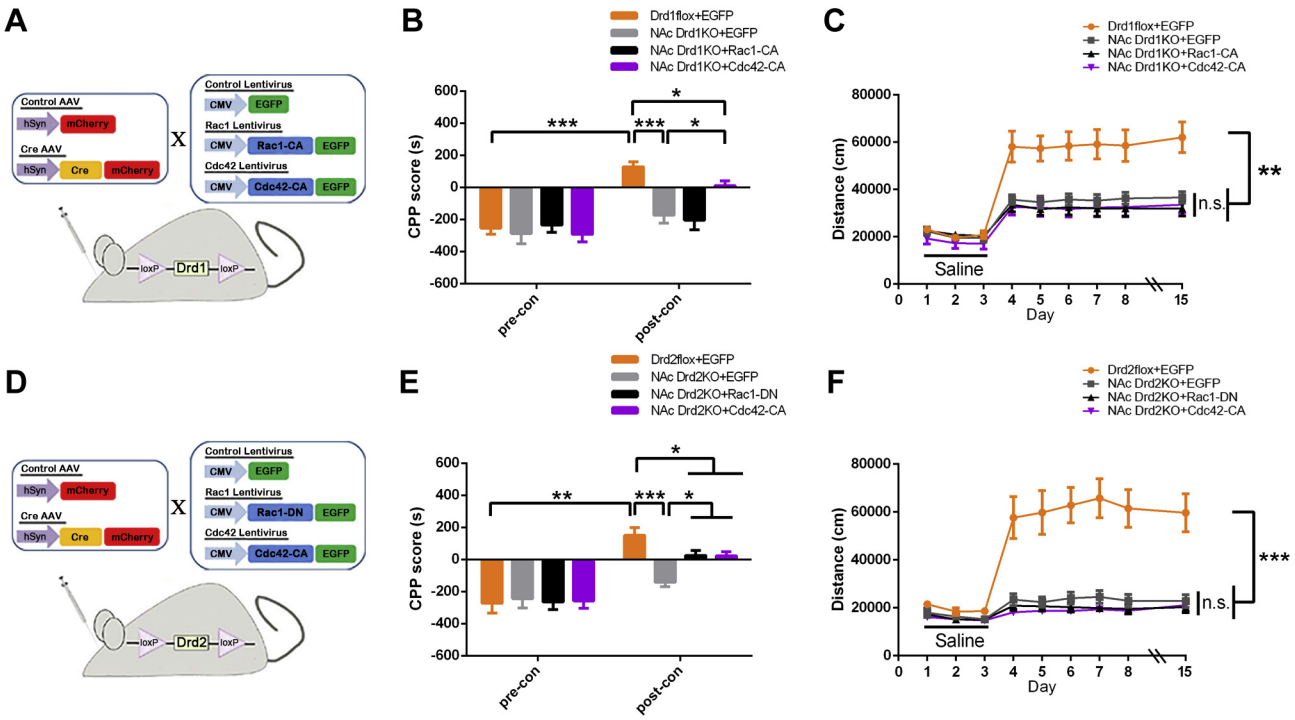

Figure 7. Dopamine D_1 and D_2 receptors (D_1Rs and D_2Rs, respectively) modulate methamphetamine (METH)-induced conditioned place preference (CPP) but not locomotor activation by differentially regulating Rac1 and Cdc42 signaling in the nucleus accumbens (NAc). **(A)** A schematic diagram of the viral vectors and transgenic mice used in this experiment. **(B)** Three weeks after stereotactic injection of the indicated viral vectors into the NAc, *Drd1*$^{loxp/loxp}$ mice were assigned to METH CPP (n = 8 or 9 mice/group). Infection with the viral vectors had no effect on basal preference during the preconditioning period. After METH CPP training, *Drd1*$^{loxp/loxp}$ mice infected with control viral vectors showed a preference for METH, which was disrupted by conditional knockout of D_1R (Drd1KO) in the NAc. Infection with a constitutively active (L61) mutant of Cdc42 (Cdc42-CA) but not Rac1 (Rac1-CA) partially restored the rewarding effect of METH in NAc Drd1KO mice. **(C)** Neither Rac1-CA nor Cdc42-CA viral vectors restored the locomotor activation induced by METH in NAc Drd1KO mice. **(D)** A schematic diagram of the viral vectors and transgenic mice used in this experiment. **(E)** Three weeks after stereotactic injection of the indicated viral vectors into the NAc, *Drd2*$^{loxp/loxp}$ mice were assigned to METH CPP (n = 7 or 8 mice/group). Infection with the viral vectors had no effect on basal preference during the preconditioning period. After METH CPP training, *Drd2*$^{loxp/loxp}$ mice infected with control viral vectors showed a preference for METH, which was disrupted by conditional knockout of D_2R (Drd2KO) in the NAc. Infection with either dominant-negative (N17) mutant of Rac1 (Rac1-DN) or Cdc42-CA partially restored the rewarding effect of METH in NAc Drd2KO mice. **(F)** Neither Rac1-DN nor Cdc42-CA restored the locomotor activation induced by METH in NAc Drd2KO mice. The data are shown as mean ± SEM. $^*p < .05$, $^{**}p < .01$, $^{***}p < .001$. AAV, adeno-associated virus; CMV, cytomegalovirus; EGFP, enhanced green fluorescent protein; n.s., not significant.

Drd2KO mice. The expression levels of total Rac1, Cdc42, PAK1, and N-WASP were unaffected in all groups (Figure 6). These data indicate that D_1Rs and D_2Rs differentially regulate Rac1 and Cdc42 signaling in the NAc after repeated METH treatment.

D_1Rs and D_2Rs Modulate METH-Induced Behavioral and Structural Plasticity by Differentially Regulating Rac1 and Cdc42 Signaling in the NAc

To evaluate whether D_1Rs and D_2Rs modulate METH-induced behavioral plasticity by regulating Rac1 and Cdc42 signaling, we modulated Rac1 and Cdc42 activity in NAc Drd1KO mice and NAc Drd2KO mice. *Drd1*$^{loxp/loxp}$ mice and *Drd2*$^{loxp/loxp}$ mice were randomly divided into four groups, and the indicated viral vectors were stereotactically injected into the NAc (Figure 7A, D). Infection with the viral vectors in *Drd1*$^{loxp/loxp}$ mice or *Drd2*$^{loxp/loxp}$ mice had no effect on the basal preference during the preconditioning period. After METH CPP training, Cdc42-CA–infected NAc Drd1KO mice showed significantly higher CPP scores than EGFP-infected NAc Drd1KO mice and lower scores than EGFP-infected *Drd1*$^{loxp/loxp}$ mice (Figure 7B). Both Rac1-DN– and Cdc42-CA–infected NAc Drd2KO mice showed significantly higher CPP scores than EGFP-infected NAc Drd2KO mice and lower scores than EGFP-infected *Drd2*$^{loxp/loxp}$ mice (Figure 7E). These results suggest that Cdc42-CA but not Rac1-CA partially restored the rewarding effect of METH in NAc Drd1KO mice. Both Rac1-DN and Cdc42-CA partially restored the rewarding effect of METH in NAc Drd2KO mice. Moreover, we found that neither Rac1-CA nor Cdc42-CA activated the locomotion of METH-treated NAc Drd1KO mice (Figure 7C) and neither Rac1-DN nor Cdc42-CA activated the locomotion of METH-treated NAc Drd2KO mice (Figure 7F).

Next, to assess whether modulating Rac1 and Cdc42 activity in NAc Drd1KO mice would ameliorate deficits in spatial learning and memory, *Drd1*$^{loxp/loxp}$ mice infected with the indicated viral vectors were subjected to the MWM experiment 7 days after METH withdrawal (Figure 8A). Compared with EGFP-infected NAc Drd1KO mice, mice infected with Rac1-CA but not Cdc42-CA exhibited shortened escape latencies and an

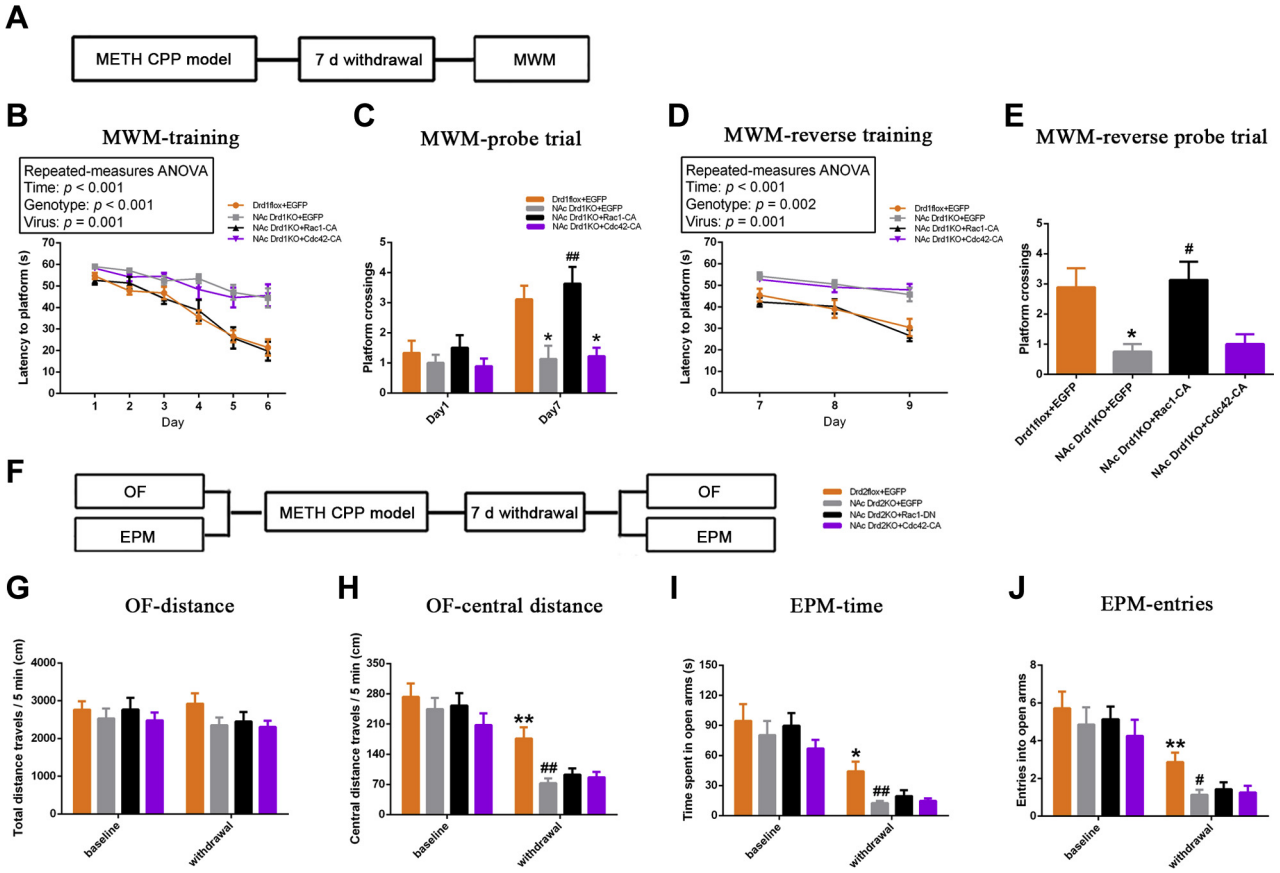

Figure 8. Dopamine D_1 and D_2 receptors (D_1Rs and D_2Rs, respectively) modulate methamphetamine (METH) withdrawal–induced spatial learning and memory impairment and anxiety-related behaviors by differentially regulating Rac1 signaling in the nucleus accumbens (NAc). **(A)** A schematic diagram of the experimental design for the Morris water maze (MWM) test in the *Drd1*$^{loxp/loxp}$ mice infected with the indicated viral vectors (n = 8 or 9 mice/group). **(B–E)** The NAc-specific conditional knockout of D_1R (NAc Drd1KO) mice infected with the constitutively active (L61) mutant of Rac1 (Rac1-CA) viral vector, but not the constitutively active (L61) mutant of Cdc42 (Cdc42-CA) viral vector, exhibited reduced METH withdrawal–induced spatial learning and memory impairment. The data are shown as mean ± SEM. Compared with Drd1flox + enhanced green fluorescent protein (EGFP) group: $^{*}p < .05$, $^{**}p < .01$; compared with NAc Drd1KO + EGFP group: $^{\#}p < .05$, $^{\#\#\#}p < .001$. **(F)** A schematic diagram of the experimental design for open field (OF) and elevated plus maze (EPM) tests in the *Drd2*$^{loxp/loxp}$ mice infected with the indicated viral vectors (n = 7 or 8 mice/group). **(G–J)** Aggravation of METH withdrawal–induced anxiety by deletion of D_2R in the NAc is Rac1 and Cdc42 signaling independent. The data are shown as mean ± SEM. Compared with baseline of Drd2flox + EGFP group: $^{*}p < .05$, $^{**}p < .01$; compared with Drd2flox + EGFP group after METH withdrawal: $^{\#}p < .05$, $^{\#\#}p < .01$. CPP, conditioned place preference; ANOVA, analysis of variance; DN, dominant-negative (N17) mutant; Drd2KO, conditional knockout of D_2 receptor.

increased number of platform crossings (Figure 8B–E). These results imply that conditional D_1R knockout aggravates spatial learning and memory impairment after METH withdrawal by inhibiting Rac1 signaling. To determine whether modulating Rac1 and Cdc42 activity in NAc Drd2KO mice would ameliorate METH withdrawal–induced anxiety, *Drd2*$^{loxp/loxp}$ mice infected with the indicated viral vectors were subjected to the OF and EPM experiments before METH CPP and 7 days after METH withdrawal (Figure 8F). The results showed that Rac1-DN– and Cdc42-CA–infected NAc Drd2KO mice exhibited similar travel distance in the central arena and similar time spent in the open arms and entries into the open arms 7 days after METH withdrawal, to EGFP-infected NAc Drd2KO mice (Figure 8G–J). These results demonstrate that neither Rac1 nor Cdc42 signaling contributes to the aggravation of anxiety-related behaviors after METH withdrawal following conditional knockout of D_2Rs in the NAc.

Finally, to confirm the connection between D_1Rs/D_2Rs and Rac1/Cdc42 in METH-induced structural plasticity, we assessed the dendritic and spine morphology of MSNs in the NAc in *Drd1*$^{loxp/loxp}$ and *Drd2*$^{loxp/loxp}$ mice infected with both the Cre viral vector and a Rac1 or Cdc42 mutant (Figure 9A). Compared with EGFP-infected NAc Drd1KO mice treated with METH, Cdc42-CA–infected NAc Drd1KO mice showed increased dendritic complexity, dendritic length, branch number, and total spine density, especially for thin and mushroom spines. In contrast, Rac1-CA–infected NAc Drd1KO mice showed no change in dendritic and spine morphology after treatment with METH (Figure 9B–K). Compared with EGFP-infected NAc Drd2KO mice treated with METH, both Rac1-DN– and Cdc42-CA–infected NAc Drd2KO mice showed increased dendritic complexity, dendritic length, branch number, and total spine density after treatment with METH. However, differences were noted between the groups, with

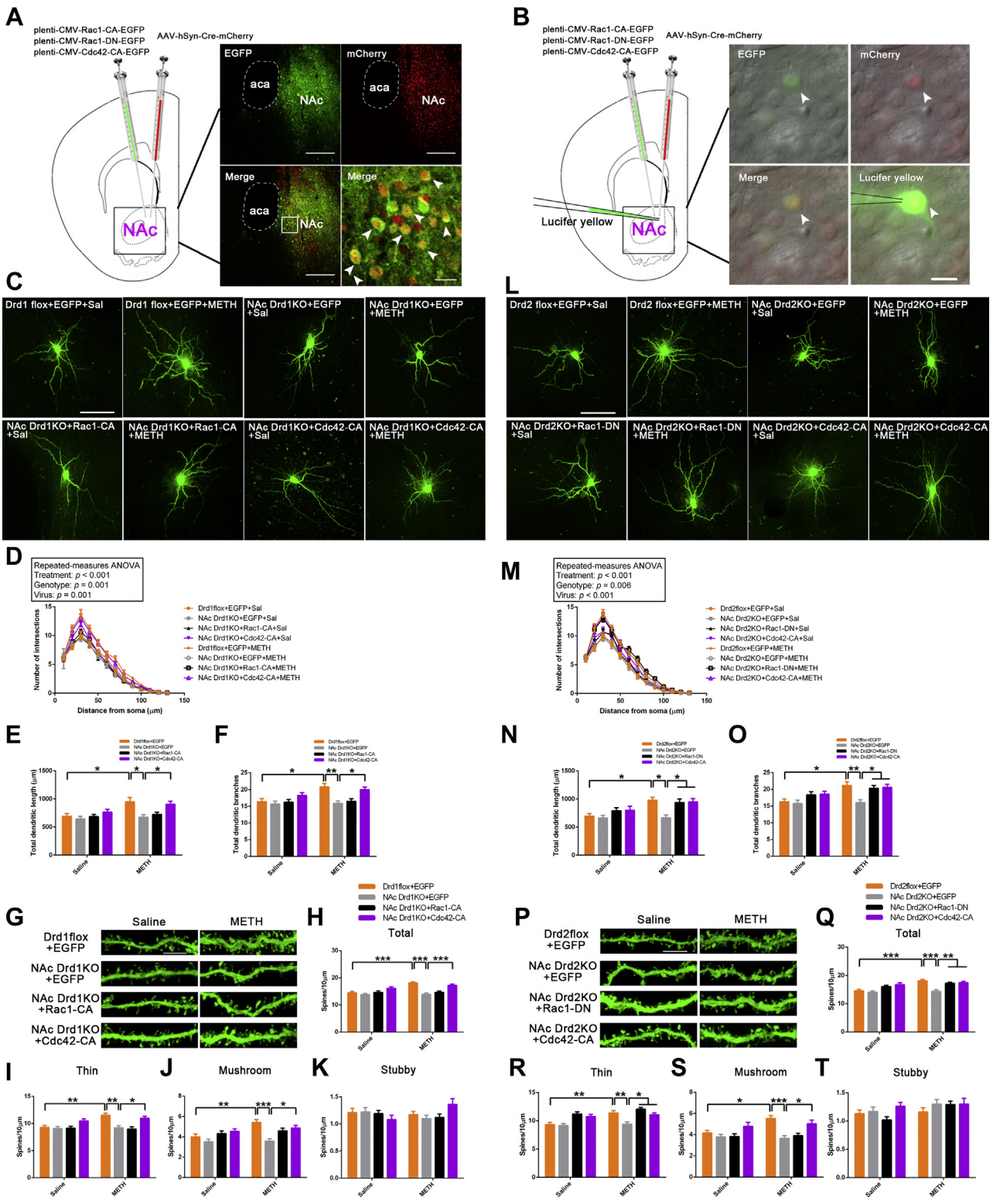

Figure 9. Dopamine D_1 and D_2 receptors (D_1Rs and D_2Rs, respectively) modulate methamphetamine (METH)-induced structural plasticity by differentially regulating Rac1 and Cdc42 signaling in the nucleus accumbens (NAc). **(A)** Representative image of the stereotactic injection site of the NAc. *Drd1*$^{loxp/loxp}$ mice and *Drd2*$^{loxp/loxp}$ mice were randomly divided into eight groups and stereotactically injected with the indicated viral vectors in the NAc. Three weeks later, the mice were assigned to saline (Sal) conditioned place preference (CPP) or METH CPP, after which coronal sections of the NAc were prepared for morphological

Rac1-DN increasing only the thin spine density and Cdc42-CA increasing the thin and mushroom spine densities (Figure 9L-T). These results suggest that D_1R activates Cdc42, whereas D_2R suppresses Rac1 and activates Cdc42 to facilitate METH-induced structural plasticity.

DISCUSSION

In the present study, we show that D_1Rs and D_2Rs in the NAc regulate METH-induced CPP, locomotor activation, and dendritic and spine remodeling of MSNs but differentially regulate METH withdrawal–induced behaviors. Interestingly, D_1R activates Rac1 and Cdc42 signaling, while D_2R inhibits Rac1 but activates Cdc42 signaling to modulate METH-induced CPP and structural plasticity but not locomotor activation. NAc D_1R deletion aggravates METH withdrawal–induced impairment of spatial learning and memory by suppressing Rac1 but not Cdc42 signaling, while NAc D_2R deletion aggravates METH withdrawal–induced anxiety through a Rac1- and Cdc42-independent signaling.

Through microinjection of the Cre virus into the NAc of *Drd1*$^{loxp/loxp}$ or *Drd2*$^{loxp/loxp}$ mice, we found that mice with conditional deletion of D_1Rs or D_2Rs in the NAc exhibited impaired METH-induced CPP and locomotor activation, which indicates that the activation of D_1Rs and D_2Rs together mediates addiction behaviors. Our results echoed those of studies showing that the excessive release of dopamine after drug administration can rapidly stimulate D_1Rs and progressively stimulate D_2Rs, causing abrupt activation of D_1-MSNs and longer-lasting deactivation of D_2-MSNs (46), thus provoking drug-evoked CPP and locomotor activation (47–49). In addition, treatment with a D_1R antagonist impairs alcohol-induced CPP (50) and METH-induced locomotion (10), whereas conditionally decreasing D_2R levels in the core of the NAc abolishes METH-induced CPP and locomotion (12). All of the above studies support our finding that D_1Rs and D_2Rs are involved in mediating METH-induced CPP and locomotor activation. Moreover, we found that conditional D_2R deletion in the NAc had a tendency to decrease locomotion, which were consistent with Sim *et al.*'s (51) report. However, how the basal locomotion changes after D_2R deletion is still controversial, which may be related to the knockout regions, experimental conditions, and sample size (12,49,51–53). A previous study showed that systemic knockout of D_1R severely impaired spatial learning and memory (43). In line with that report, we found that D_1R plays an important role in spatial learning and memory. Compared with NAc D_2-MSNs, NAc D_1-MSNs receive stronger inputs from the ventral hippocampus, which supplies information regarding spatial and contextual values (47,54). The conditional D_1R deletion in the NAc may mimic the attenuated mesolimbic dopamine signaling that mediates spatial learning and memory after METH withdrawal. Moreover, both clinical and animal experiments found that striatal D_2R levels are significantly reduced after drug withdrawal (55,56). Increasing D_2R levels but not D_1R levels prevent the aversive symptoms of drug withdrawal (57). Another study showed that D_2R deletion did not affect anxiety-related behaviors under basal conditions; however, the anxiety-related behaviors were increased after exposure to stress (51). These reports support our finding that conditional D_2R deletion had no effect on animal's anxiety-related behaviors under saline treatment but severely increased METH withdrawal–induced anxiety. Together, our results indicate that D_1Rs and D_2Rs can consistently or differentially mediate METH-associated behaviors.

The structural hallmarks of MSNs in the NAc are complex dendritic branches and abundant dendritic spines; these branches and spines are susceptible to morphological changes after drug exposure (23–25). After METH CPP training, we observed more complex dendrites, increased dendritic length and branching, and augmented dendritic spine density, especially for thin and mushroom spines. Our results are consistent with a previous observation that the densities of both thin and mushroom spines are increased in the dorsolateral caudate putamen after METH treatment (58). D_1Rs and D_2Rs facilitate spine formation in cultured striatal MSNs (59) and are critical for spine remodeling induced by other psychological disorders, such as stress and schizophrenia (60,61). D_1R promotes the increase in dendritic branches and spine density induced by cocaine, and D_2R is involved in the regulation of dendritic complexity (23,28). In line with these reports, our results show that conditional D_1R or D_2R deletion in the NAc suppresses the METH-induced increases in dendritic complexity, dendritic length, branch number, and total spine density. The decrease in total spines was largely driven by the reduced number of thin and mushroom spines. Our results suggest that both D_1Rs and D_2Rs are involved in METH-induced structural plasticity. As membrane surface receptors, dopamine receptors must cooperate with intracellular

observation. The arrowheads indicate the medium spiny neurons (MSNs) expressing both enhanced green fluorescent protein (EGFP) and mCherry. Scale bar = 200 μm or 10 μm. **(B)** A schematic diagram of Lucifer yellow intracellular injection experiment. Only MSNs expressing both EGFP and mCherry in the NAc were selected for intracellular injection of Lucifer yellow, as the arrowheads show. Scale bar = 10 μm. **(C, L)** Representative morphology of MSNs in each group. The images were obtained by confocal scanning at the specific excitation wavelength (405 nm) of Lucifer yellow (n = 15–21 neurons/group, sampled from 3 mice/treatment condition). Scale bar = 50 μm. **(D–F)** METH-induced increases in dendritic complexity, dendritic length, and branch number were blocked in NAc-specific conditional knockout of D_1R (NAc Drd1KO) mice but were restored by constitutively active (L61) mutant of Cdc42 (Cdc42-CA) viral vector infection. **(G, P)** Representative images of dendritic spines in each group (n = 19–27 dendrites/group, sampled from 3 mice/treatment condition). Only dendrites from MSNs expressing both EGFP and mCherry in the NAc were selected. Scale bar = 5 μm. **(H)** The METH-induced increase in total spine density was blocked in NAc Drd1KO mice but was restored by Cdc42-CA viral vector infection. **(I–K)** The spine density increase following Cdc42-CA infection of NAc Drd1KO mice treated with METH was largely driven by the increase in thin and mushroom spines. **(M–O)** METH-induced increases in dendritic complexity, dendritic length, and branch number were blocked in NAc-specific conditional knockout of D_2R (NAc Drd2KO) mice but were restored by dominant-negative (N17) mutant of Rac1 (Rac1-DN) or Cdc42-CA viral vector infection. **(Q)** The METH-induced increase in total spine density was blocked in NAc Drd2KO mice but was restored by Rac1-DN or Cdc42-CA viral vector infection. **(R–T)** The increase in spine density following Rac1-DN infection in NAc Drd2KO mice treated with METH was largely driven by an increase in thin spines. In contrast, Cdc42-CA increased the numbers of both thin and mushroom spines. None of the viral vectors had an effect on stubby spine density. The data are shown as mean ± SEM. $^*p < .05$, $^{**}p < .01$, $^{***}p < .001$. AAV, adeno-associated virus; ANOVA, analysis of variance; CMV, cytomegalovirus.

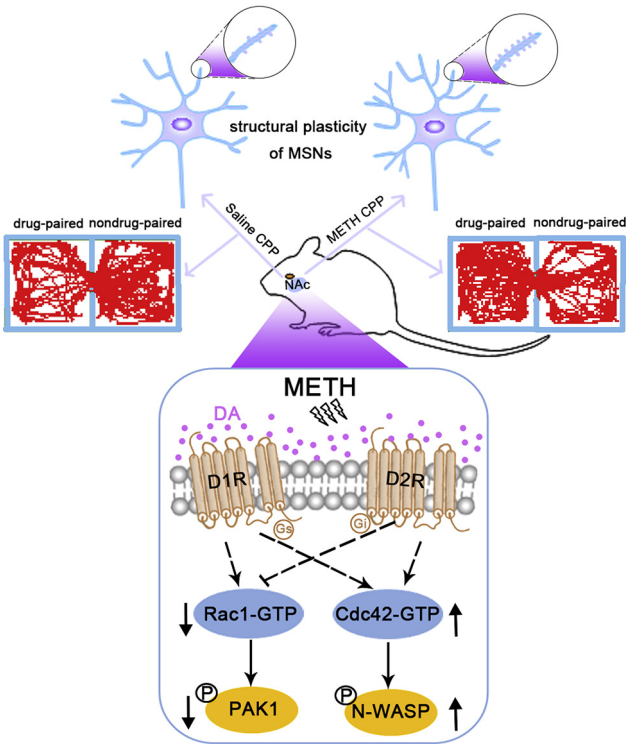

Figure 10. Summary: dopamine D_1 and D_2 receptors (D_1Rs and D_2Rs, respectively) in the nucleus accumbens (NAc) differentially regulate Rac1 and Cdc42 signaling to modulate methamphetamine (METH)-induced behavioral and structural plasticity. CPP, conditioned place preference; DA, dopamine; GTP, guanosine triphosphate; MSNs, medium spiny neurons; N-WASP, neural Wiskott–Aldrich syndrome protein; PAK1, p21 (Rac1) activated kinase 1.

molecules to modulate structural remodeling. Rac1 and Cdc42 are the two key molecules involved in regulating dendritic growth and spine remodeling (29,31,32). Rac1 activation can promote dendritic growth and spine formation (29,33) while suppressing the growth of axons (62). In addition, our team reported that Rac1 activation in the caudate putamen mediates a cocaine-induced increase in spine density (35), while Dietz *et al.* (20) reported that Rac1 inactivation in the NAc also increases spine density after repeated cocaine administration. These studies indicate that Rac1 plays complex and differential roles in structural remodeling depending on the subcellular structure and brain region. In our study, Rac1 signaling, including Rac1 activity and PAK1 phosphorylation, was suppressed in the NAc after repeated METH treatment, and the suppression of Rac1 activity was responsible for METH-induced dendritic remodeling and increased thin spine density. Our results are in line with previous findings regarding Rac1 in the NAc after cocaine treatment, which showed that decreased Rac1 signaling may mediate actin nucleation and filament assembly to promote thin spine formation through the PAK1-cofilin pathway (20,63). Our results also showed that METH increased Cdc42 signaling, including Cdc42 activity and N-WASP phosphorylation; this result was inconsistent with Dietz *et al.*'s (20) report. Cdc42 activation promotes dendritic growth and spine formation (29,30), while conditional Cdc42 deletion induces spine loss (34). Consistent with these reports, we found that Cdc42 activation increased the densities of thin and mushroom spines, and Cdc42 inactivation suppressed the METH-induced dendritic and spine remodeling. These results indicate that Cdc42 activation may be critical for METH-induced dendritic growth and spine formation. This conclusion is supported by previous reports showing that Cdc42 signaling can mediate actin branching and spine head enlargement through the N-WASP-Arp2/3 pathway (31,64). However, we cannot rule out the possibility that the activities of PAK1 and N-WASP are coregulated by Rac1 and Cdc42, which is a subject of our future investigation.

Dopamine receptors participate in a variety of biological processes, such as active forgetting, dendritic remodeling, and gene expression, by regulating the Rho family GTPases (37–39). Here, we showed that D_1R activates Rac1 and Cdc42 signaling, whereas D_2R inhibits Rac1 but activates Cdc42 signaling to modulate METH-induced CPP and structural plasticity. Our findings are reminiscent of a recent study showing that in *Drosophila*, two different dopamine receptors, dDA1 and DAMB, are required for different aspects of memory. Specifically, whereas dDA1 mediates acquisition, DAMB mediates forgetting (65,66). The activation of Rac1 mediates forgetting, whereas the activation of Cdc42 promotes both memory acquisition and forgetting (66–68). Moreover, the DAMB receptor mediates active forgetting by activating Rac-cofilin signaling (37). These investigations indicate that the differential regulation of Rac1 and Cdc42 signaling by D_1Rs and D_2Rs may mediate different aspects of METH-associated memory, which is usually evaluated using the CPP model (69–71). The possible explanation of our findings is that, on the one hand, the rapid stimulation of D_1R activates Rac1 to trigger active forgetting, whereas the progressive stimulation of D_2R inactivates Rac1 to slow the decay of memory (46). On the other hand, D_1Rs and D_2Rs consistently activate Cdc42 to promote both memory acquisition and forgetting (66), ultimately leading to the consolidation, not the decay, of METH-associated memory. The observed METH-induced CPP and structural plasticity may be manifestations of drug-associated pathological memory, which usurps the similar mechanism of normal learning and memory to inhibit active forgetting, thus prolonging memory (44). Similar to research describing how an *N*-methyl-D-aspartate antagonist disrupts cocaine-induced CPP but spares locomotor activation (72) and research showing that restraint stress reduces METH-induced CPP without impairing locomotor sensitization (73), our results reveal that interfering with Rac1 and Cdc42 affects METH-induced CPP but not locomotor activation. These data highlight the complex signaling pathways involved in METH-induced CPP and locomotor activation. METH-induced locomotor activation might be mediated by other D_1R and D_2R downstream effectors, such as extracellular signal-related kinase, protein kinase B, dopamine and cyclic adenosine monophosphate-regulated phosphoprotein Mr 32 kDa, and ΔFosB (74,75). In addition, we found that Rac1, but not Cdc42, might act downstream of D_1Rs to mediate spatial learning and memory, which is consistent with previous findings that deficient Rac1-PAK signaling impairs spatial learning and memory consolidation (76,77). Another study reported that the inhibition of hippocampal Cdc42 activity increases anxiety (78). We found that D_2R deletion in the NAc aggravates

METH withdrawal–induced anxiety through a Rac1- and Cdc42-independent signaling mechanism, exemplifying the complexity of the pathways that mediate anxiety in different brain regions.

In conclusion, D_1Rs and D_2Rs in the NAc differentially regulate Rac1 and Cdc42 signaling to modulate METH-induced CPP and structural plasticity but not locomotor activation (Figure 10). Additionally, D_1R alleviates METH withdrawal–induced spatial learning and memory impairment through Rac1 signaling activation but not Cdc42 signaling, whereas D_2R alleviates METH withdrawal–induced anxiety without affecting Rac1 or Cdc42 signaling. Our findings suggest that the dopamine receptor signaling to downstream molecules, such as Rac1 and/or Cdc42, may serve as a therapeutic target for the treatment of drug addiction.

ACKNOWLEDGMENTS AND DISCLOSURES

This work was supported by Natural Science Foundation of China Grant Nos. 81571860 (to LuZ), 81430045 (to HW), and 81872514 (to LiZ); Colleges Pearl River Scholar Funded Scheme Grant No. GDUPS2015 (to LuZ); Natural Science Foundation of Guangdong Province Grant Nos. 2018B030311062 (to LuZ) and 2014A030312013 (to LiZ); and Program for Changjiang Scholars and Innovative Research Team in University Grant No. IRT 16R37 (to TG).

The authors report no biomedical financial interests or potential conflicts of interest.

ARTICLE INFORMATION

From the Key Laboratory of Functional Proteomics of Guangdong Province (GT, LYi, LYe, JZ, YL, MZ, YW, BX, HG, LuZ), Key Laboratory of Construction and Detection in Tissue Engineering of Guangdong Province (JL, LiZ), and Key Laboratory of Mental Health of the Ministry of Education (LuZ), School of Basic Medical Sciences; School of Forensic Medicine (HW); and Institute of Comparative Medicine and Laboratory Animal Center (NL), Southern Medical University, Guangzhou, China; and Division of Experimental Hematology and Cancer Biology (FG), Children's Hospital Research Foundation, Cincinnati, Ohio.

Address correspondence to Lin Zhang, M.D., Ph.D., Key Laboratory of Construction and Detection in Tissue Engineering of Guangdong Province, School of Basic Medical Sciences, Southern Medical University, 1023 Shatainan Road, Baiyun District, Guangzhou 510515, China; E-mail: zlilyzh@126.com; or Lu Zhang, M.D., Ph.D., Key Laboratory of Functional Proteomics of Guangdong Province, Key Laboratory of Mental Health of the Ministry of Education, School of Basic Medical Sciences, Southern Medical University, 1023 Shatainan Road, Baiyun District, Guangzhou 510515, China; E-mail: zlulu70@126.com.

Received Oct 31, 2018; revised Feb 21, 2019; accepted Mar 3, 2019.

Supplementary material cited in this article is available online at https://doi.org/10.1016/j.biopsych.2019.03.966.

REFERENCES

1. Koob GF, Volkow ND (2009): Neurocircuitry of addiction. Neuropsychopharmacology 35:217–238.
2. Arias-Carrion O, Stamelou M, Murillo-Rodriguez E, Menendez-Gonzalez M, Poppel E (2010): Dopaminergic reward system: A short integrative review. Int Arch Med 3:24.
3. Di Chiara G, Bassareo V, Fenu S, De Luca MA, Spina L, Cadoni C, *et al.* (2004): Dopamine and drug addiction: The nucleus accumbens shell connection. Neuropharmacology 47(suppl 1):227–241.
4. Hyman SE (2005): Addiction: A disease of learning and memory. Am J Psychiatry 162:1414–1422.
5. Juarez B, Han MH (2016): Diversity of dopaminergic neural circuits in response to drug exposure. Neuropsychopharmacology 41:2424–2446.
6. Nestler EJ, Lobo MK (2011): The striatal balancing act in drug addiction: Distinct roles of direct and indirect pathway medium spiny neurons. Front Neuroanat 5:41.
7. Yao WD, Gainetdinov RR, Arbuckle MI, Sotnikova TD, Cyr M, Beaulieu JM, *et al.* (2004): Identification of PSD-95 as a regulator of dopamine-mediated synaptic and behavioral plasticity. Neuron 41:625–638.
8. Badiani A, Robinson TE (2004): Drug-induced neurobehavioral plasticity: The role of environmental context. Behav Pharmacol 15:327–339.
9. Bertran-Gonzalez J, Bosch C, Maroteaux M, Matamales M, Herve D, Valjent E, *et al.* (2008): Opposing patterns of signaling activation in dopamine D1 and D2 receptor-expressing striatal neurons in response to cocaine and haloperidol. J Neurosci 28:5671–5685.
10. Hall DA, Powers JP, Gulley JM (2009): Blockade of D1 dopamine receptors in the medial prefrontal cortex attenuates amphetamine- and methamphetamine-induced locomotor activity in the rat. Brain Res 1300:51–57.
11. Carati C, Schenk S (2011): Role of dopamine D1- and D2-like receptor mechanisms in drug-seeking following methamphetamine self-administration in rats. Pharmacol Biochem Behav 98:449–454.
12. Miyamoto Y, Iida A, Sato K, Muramatsu Si, Nitta A (2014): Knockdown of dopamine D2 receptors in the nucleus accumbens core suppresses methamphetamine-induced behaviors and signal transduction in mice. Int J Neuropsychopharmacol 18:pyu038.
13. Mizoguchi H, Yamada K, Mizuno M, Mizuno T, Nitta A, Noda Y, *et al.* (2004): Regulations of methamphetamine reward by extracellular signal-regulated kinase 1/2/ets-like gene-1 signaling pathway via the activation of dopamine receptors. Mol Pharmacol 65:1293–1301.
14. Kuhar MJ, Pilotte NS (1996): Neurochemical changes in cocaine withdrawal. Trends Pharmacol Sci 17:260–264.
15. Puig S, Marie N, Benturquia N, Noble F (2014): Influence of cocaine administration patterns on dopamine receptor regulation. Psychopharmacology 231:3131–3137.
16. Radke AK, Gewirtz JC (2012): Increased dopamine receptor activity in the nucleus accumbens shell ameliorates anxiety during drug withdrawal. Neuropsychopharmacology 37:2405–2415.
17. Amin B, Andalib S, Vaseghi G, Mesripour A (2016): Learning and memory performance after withdrawal of agent abuse: A review. Iran J Psychiatry Behav Sci 10:e1822.
18. Nagai T, Takuma K, Dohniwa M, Ibi D, Mizoguchi H, Kamei H, *et al.* (2007): Repeated methamphetamine treatment impairs spatial working memory in rats: Reversal by clozapine but not haloperidol. Psychopharmacology 194:21–32.
19. Li J, Liu N, Lu K, Zhang L, Gu J, Guo F, *et al.* (2012): Cocaine-induced dendritic remodeling occurs in both D1 and D2 dopamine receptor-expressing neurons in the nucleus accumbens. Neurosci Lett 517:118–122.
20. Dietz DM, Sun H, Lobo MK, Cahill ME, Chadwick B, Gao V, *et al.* (2012): Rac1 is essential in cocaine-induced structural plasticity of nucleus accumbens neurons. Nat Neurosci 15:891–896.
21. Williams MT, Brown RW, Vorhees CV (2004): Neonatal methamphetamine administration induces region-specific long-term neuronal morphological changes in the rat hippocampus, nucleus accumbens and parietal cortex. Eur J Neurosci 19:3165–3170.
22. Golden SA, Russo SJ (2012): Mechanisms of psychostimulant-induced structural plasticity. Cold Spring Harb Perspect Med 2:a011957.
23. Zhang L, Huang L, Lu K, Liu Y, Tu G, Zhu M, *et al.* (2017): Cocaine-induced synaptic structural modification is differentially regulated by dopamine D1 and D3 receptors-mediated signaling pathways. Addict Biol 22:1842–1855.
24. Ceglia I, Lee KW, Cahill ME, Graves SM, Dietz D, Surmeier DJ, *et al.* (2017): WAVE1 in neurons expressing the D1 dopamine receptor regulates cellular and behavioral actions of cocaine. Proc Natl Acad Sci U S A 114:1395–1400.
25. Pulipparacharuvil S, Renthal W, Hale CF, Taniguchi M, Xiao G, Kumar A, *et al.* (2008): Cocaine regulates MEF2 to control synaptic and behavioral plasticity. Neuron 59:621–633.
26. Ehlinger DG, Burke JC, McDonald CG, Smith RF, Bergstrom HC (2017): Nicotine-induced and D1-receptor-dependent dendritic

remodeling in a subset of dorsolateral striatum medium spiny neurons. Neuroscience 356:242–254.
27. Wang J, Cheng Y, Wang X, Roltsch Hellard E, Ma T, Gil H, *et al.* (2015): Alcohol elicits functional and structural plasticity selectively in dopamine D1 receptor-expressing neurons of the dorsomedial striatum. J Neurosci 35:11634–11643.
28. Ren Z, Sun WL, Jiao H, Zhang D, Kong H, Wang X, *et al.* (2010): Dopamine D1 and N-methyl-D-aspartate receptors and extracellular signal-regulated kinase mediate neuronal morphological changes induced by repeated cocaine administration. Neuroscience 168:48–60.
29. Threadgill R, Bobb K, Ghosh A (1997): Regulation of dendritic growth and remodeling by Rho, Rac, and Cdc42. Neuron 19:625–634.
30. Tashiro A, Minden A, Yuste R (2000): Regulation of dendritic spine morphology by the rho family of small GTPases: Antagonistic roles of Rac and Rho. Cereb Cortex 10:927–938.
31. Murakoshi H, Wang H, Yasuda R (2011): Local, persistent activation of Rho GTPases during plasticity of single dendritic spines. Nature 472:100–104.
32. Hedrick NG, Harward SC, Hall CE, Murakoshi H, McNamara JO, Yasuda R (2016): Rho GTPase complementation underlies BDNF-dependent homo- and heterosynaptic plasticity. Nature 538:104–108.
33. Nakayama AY, Harms MB, Luo L (2000): Small GTPases Rac and Rho in the maintenance of dendritic spines and branches in hippocampal pyramidal neurons. J Neurosci 20:5329–5338.
34. Kim IH, Wang H, Soderling SH, Yasuda R (2014): Loss of Cdc42 leads to defects in synaptic plasticity and remote memory recall. eLife 3:02839.
35. Li J, Zhang L, Chen Z, Xie M, Huang L, Xue J, *et al.* (2015): Cocaine activates Rac1 to control structural and behavioral plasticity in caudate putamen. Neurobiol Dis 75:159–176.
36. Mizuo K, Katada R, Okazaki S, Tateda K, Watanabe S, Matsumoto H (2012): Epigenetic regulation of MIR-124 under ethanol dependence and withdrawal. Nihon Arukoru Yakubutsu Igakkai Zasshi 47:155–163.
37. Cervantes-Sandoval I, Chakraborty M, MacMullen C, Davis RL (2016): Scribble scaffolds a signalosome for active forgetting. Neuron 90:1230–1242.
38. Li J, Gu J, Wang B, Xie M, Huang L, Liu Y, *et al.* (2015): Activation of dopamine D1 receptors regulates dendritic morphogenesis through Rac1 and RhoA in prefrontal cortex neurons. Mol Neurobiol 51:1024–1037.
39. Ho G, Wang Y, Jones PG, Young KH (2007): Activation of serum response element by D2 dopamine receptor is governed by Gβγ-mediated MAPK and rho pathways and regulated by RGS proteins. Pharmacology 79:114–121.
40. Barr AM, Panenka WJ, MacEwan GW, Thornton AE, Lang DJ, Honer WG, *et al.* (2006): The need for speed: An update on methamphetamine addiction. J Psychiatry Neurosci 31:301–313.
41. Gould TD, Dao DT, Kovacsics CE (2009): The open field test. In: Gould TD editor. Mood and Anxiety Related Phenotypes in Mice: Characterization Using Behavioral Tests. Totowa, NJ: Humana Press, 1–20.
42. Walf AA, Frye CA (2007): The use of the elevated plus maze as an assay of anxiety-related behavior in rodents. Nat Protoc 2:322–328.
43. Granado N, Ortiz O, Suarez LM, Martin ED, Cena V, Solis JM, *et al.* (2008): D1 but not D5 dopamine receptors are critical for LTP, spatial learning, and LTP-Induced arc and zif268 expression in the hippocampus. Cereb Cortex 18:1–12.
44. Young EJ, Aceti M, Griggs EM, Fuchs RA, Zigmond Z, Rumbaugh G, *et al.* (2014): Selective, retrieval-independent disruption of methamphetamine-associated memory by actin depolymerization. Biol Psychiatry 75:96–104.
45. Muñoz-Cuevas FJ, Athilingam J, Piscopo D, Wilbrecht L (2013): Cocaine-induced structural plasticity in frontal cortex correlates with conditioned place preference. Nat Neurosci 16:1367–1369.
46. Luo Z, Volkow ND, Heintz N, Pan Y, Du C (2011): Acute cocaine induces fast activation of D1 receptor and progressive deactivation of D2 receptor striatal neurons: In vivo optical microprobe [Ca2+]i imaging. J Neurosci 31:13180–13190.
47. Kim HJ, Lee JH, Yun K, Kim JH (2017): Alterations in striatal circuits underlying addiction-like behaviors. Mol Cells 40:379–385.
48. Durieux PF, Bearzatto B, Guiducci S, Buch T, Waisman A, Zoli M, *et al.* (2009): D2R striatopallidal neurons inhibit both locomotor and drug reward processes. Nat Neurosci 12:393–395.
49. Kharkwal G, Radl D, Lewis R, Borrelli E (2016): Dopamine D2 receptors in striatal output neurons enable the psychomotor effects of cocaine. Proc Natl Acad Sci U S A 113:11609–11614.
50. Pina MM, Cunningham CL (2014): Effects of dopamine receptor antagonists on the acquisition of ethanol-induced conditioned place preference in mice. Psychopharmacology 231:459–468.
51. Sim HR, Choi TY, Lee HJ, Kang EY, Yoon S, Han PL, *et al.* (2013): Role of dopamine D2 receptors in plasticity of stress-induced addictive behaviours. Nat Commun 4:1579.
52. Bello EP, Casas-Cordero R, Galiñanes GL, Casey E, Belluscio MA, Rodríguez V, *et al.* (2016): Inducible ablation of dopamine D2 receptors in adult mice impairs locomotion, motor skill learning and leads to severe parkinsonism. Mol Psychiatry 22:595–604.
53. Welter M, Vallone D, Samad TA, Meziane H, Usiello A, Borrelli E (2007): Absence of dopamine D2 receptors unmasks an inhibitory control over the brain circuitries activated by cocaine. Proc Natl Acad Sci U S A 104:6840–6845.
54. Cooper S, Robison AJ, Mazei-Robison MS (2017): Reward circuitry in addiction. Neurotherapeutics 14:687–697.
55. Kohno M, Okita K, Morales AM, Robertson CL, Dean AC, Ghahremani DG, *et al.* (2016): Midbrain functional connectivity and ventral striatal dopamine D2-type receptors: Link to impulsivity in methamphetamine users. Mol Psychiatry 21:1554–1560.
56. Wolf ME (2016): Synaptic mechanisms underlying persistent cocaine craving. Nat Rev Neurosci 17:351–365.
57. Grieder TE, George O, Tan H, George SR, Le Foll B, Laviolette SR, *et al.* (2012): Phasic D1 and tonic D2 dopamine receptor signaling double dissociate the motivational effects of acute nicotine and chronic nicotine withdrawal. Proc Natl Acad Sci U S A 109:3101–3106.
58. Jedynak JP, Uslaner JM, Esteban JA, Robinson TE (2007): Methamphetamine-induced structural plasticity in the dorsal striatum. Eur J Neurosci 25:847–853.
59. Fasano C, Bourque MJ, Lapointe G, Leo D, Thibault D, Haber M, *et al.* (2013): Dopamine facilitates dendritic spine formation by cultured striatal medium spiny neurons through both D1 and D2 dopamine receptors. Neuropharmacology 67:432–443.
60. Lin GL, Borders CB, Lundewall LJ, Wellman CL (2015): D1 receptors regulate dendritic morphology in normal and stressed prelimbic cortex. Psychoneuroendocrinology 51:101–111.
61. Castillo-Gomez E, Varea E, Blasco-Ibanez JM, Crespo C, Nacher J (2016): Effects of chronic dopamine D2R agonist treatment and polysialic acid depletion on dendritic spine density and excitatory neurotransmission in the mPFC of adult rats. Neural Plast 2016:1615363.
62. Luo L, Hensch TK, Ackerman L, Barbel S, Jan LY, Jan YN (1996): Differential effects of the Rac GTPase on Purkinje cell axons and dendritic trunks and spines. Nature 379:837–840.
63. Andrianantoandro E, Pollard TD (2006): Mechanism of actin filament turnover by severing and nucleation at different concentrations of ADF/cofilin. Mol Cell 24:13–23.
64. Wegner AM, Nebhan CA, Hu L, Majumdar D, Meier KM, Weaver AM, *et al.* (2008): N-wasp and the arp2/3 complex are critical regulators of actin in the development of dendritic spines and synapses. J Biol Chem 283:15912–15920.
65. Himmelreich S, Masuho I, Berry JA, MacMullen C, Skamangas NK, Martemyanov KA, *et al.* (2017): Dopamine receptor DAMB signals via Gq to mediate forgetting in drosophila. Cell Rep 21:2074–2081.
66. Davis RL, Zhong Y (2017): The biology of forgetting-a perspective. Neuron 95:490–503.
67. Zhang X, Li Q, Wang L, Liu ZJ, Zhong Y (2016): Cdc42-dependent forgetting regulates repetition effect in prolonging memory retention. Cell Rep 16:817–825.

68. Shuai Y, Lu B, Hu Y, Wang L, Sun K, Zhong Y (2010): Forgetting is regulated through Rac activity in Drosophila. Cell 140:579–589.
69. Otis JM, Mueller D (2017): Reversal of cocaine-associated synaptic plasticity in medial prefrontal cortex parallels elimination of memory retrieval. Neuropsychopharmacology 42:2000–2010.
70. Aguilar-Valles A, Vaissiere T, Griggs EM, Mikaelsson MA, Takacs IF, Young EJ, *et al.* (2014): Methamphetamine-associated memory is regulated by a writer and an eraser of permissive histone methylation. Biol Psychiatry 76:57–65.
71. Kelley AE (2004): Memory and addiction. Neuron 44:161–179.
72. Carmack SA, Kim JS, Sage JR, Thomas AW, Skillicorn KN, Anagnostaras SG (2013): The competitive NMDA receptor antagonist CPP disrupts cocaine-induced conditioned place preference, but spares behavioral sensitization. Behav Brain Res 239:155–163.
73. Seo J-Y, Ko Y-H, Ma S-X, Lee B-R, Lee S-Y, Jang C-G (2018): Repeated restraint stress reduces the acquisition and relapse of methamphetamine-conditioned place preference but not behavioral sensitization. Brain Res Bull 139:99–104.
74. Hasbi A, Perreault ML, Shen MYF, Fan T, Nguyen T, Alijaniaram M, *et al.* (2017): Activation of dopamine D1-D2 receptor complex attenuates cocaine reward and reinstatement of cocaine-seeking through inhibition of DARPP-32, ERK, and DeltaFosB. Front Pharmacol 8:924.
75. Shi X, McGinty JF (2011): D1 and D2 dopamine receptors differentially mediate the activation of phosphoproteins in the striatum of amphetamine-sensitized rats. Psychopharmacology 214:653–663.
76. Haditsch U, Leone DP, Farinelli M, Chrostek-Grashoff A, Brakebusch C, Mansuy IM, *et al.* (2009): A central role for the small GTPase Rac1 in hippocampal plasticity and spatial learning and memory. Mol Cell Neurosci 41:409–419.
77. Hayashi ML, Choi SY, Rao BS, Jung HY, Lee HK, Zhang D, *et al.* (2004): Altered cortical synaptic morphology and impaired memory consolidation in forebrain- specific dominant-negative PAK transgenic mice. Neuron 42:773–787.
78. Hanin G, Shenhar-Tsarfaty S, Yayon N, Yau YH, Bennett ER, Sklan EH, *et al.* (2014): Competing targets of microRNA-608 affect anxiety and hypertension. Hum Mol Genet 23:4569–4580.